

UC San Diego

UC San Diego Previously Published Works

Title

Water phase transition and signal nulling in 3D dual-echo adiabatic inversion-recovery UTE (IR-UTE) imaging of myelin

Permalink

<https://escholarship.org/uc/item/2mn5m9dz>

Journal

Magnetic Resonance in Medicine, 92(6)

ISSN

0740-3194

Authors

Athertya, Jiyo S

Shin, Soo Hyun

Malhi, Bhavsimran Singh

et al.

Publication Date

2024-12-01

DOI

10.1002/mrm.30243

Peer reviewed

Water phase transition and signal nulling in 3D dual-echo adiabatic inversion-recovery UTE (IR-UTE) imaging of myelin

Jiyo S. Athertya¹  | Soo Hyun Shin¹  | Bhavsimran Singh Malhi¹ | James Lo^{1,2} | Sam Sedaghat³ | Hyungseok Jang⁴  | Yajun Ma¹  | Jiang Du^{1,5}

¹Department of Radiology, University of California, San Diego, California USA

²Department of Bioengineering, University of California, San Diego, California USA

³Department of Diagnostic and Interventional Radiology, University Hospital Heidelberg, Heidelberg, Germany

⁴Department of Radiology, University of California, Davis, California USA

⁵Radiology Service, Veterans Affairs San Diego Healthcare System, San Diego, California USA

Correspondence

Jiang Du, Department of Radiology, University of California, San Diego, 9452 Medical Center Dr., San Diego, CA 92037. Email: jiangdu@health.ucsd.edu

Funding information

Clinical Science Research & Development, Grant/Award Number: I01CX002211; National Institutes of Health, Grant/Award Numbers: F32AG082458, RF1 AG075717

Abstract

Purpose: The semisolid myelin sheath has very fast transverse relaxation and is invisible to conventional MRI sequences. UTE sequences can detect signal from myelin. The major challenge is the concurrent detection of various water components.

Methods: The inversion recovery (IR)-based UTE (IR-UTE) sequence employs an adiabatic inversion pulse to invert and suppress water magnetizations. TI plays a key role in water suppression, with negative water magnetizations (negative phase) before the null point and positive water magnetizations (positive phase) after the null point. A series of dual-echo IR-UTE images were acquired with different TIs to detect water phase transition. The effects of TR in phase transition and water suppression were also investigated using a relatively long TR of 500 ms and a short TR of 106 ms. The water phase transition in dual-echo IR-UTE imaging of myelin was investigated in five ex vivo and five in vivo human brains.

Results: An apparent phase transition was observed in the second echo at the water signal null point, where the myelin signal was selectively detected by the UTE data acquisition at the optimal TI. The water phase transition point varied significantly across the brain when the long TR of 500 ms was used, whereas the convergence of TIs was observed when the short TR of 106 ms was used.

Conclusion: The results suggest that the IR-UTE sequence with a short TR allows uniform inversion and nulling of water magnetizations, thereby providing volumetric imaging of myelin.

KEYWORDS

MRI, myelin, phase transition, UTE, white matter

1 | INTRODUCTION

Myelin sheath is a multilamellar membrane consisting of alternating protein and lipid layers that insulate axons against electrical activity.¹ Myelin damage disrupts axonal transport, integrity, and structural plasticity; reduces signal transduction; and deranges many aspects of neurological function, including speech, balance, and cognitive awareness.^{2–4} Myelin loss is central to understanding the disability seen in many neurological diseases. Noninvasive magnetic MRI of myelin could be critical in providing a more precise diagnosis of demyelinating disorders and monitoring demyelination and remyelination during treatment.^{5–7}

The semisolid myelin sheath has very fast transverse relaxation, with T_2 or T_2^* on the order of hundreds of microseconds or less.^{8–10} As a result, myelin is invisible with conventional MRI sequences, which typically have TEs of several milliseconds or longer. Conventional MRI techniques allow indirect imaging of myelin with signals from intracellular and extracellular water as well as CSF.^{5–7} Whereas conventional MRI techniques are highly effective in showing focal lesions, they lack sensitivity and specificity to diffuse changes in normal-appearing white matter, such as partial myelin loss.¹¹ In other words, conventional MRI sequences have difficulty mapping myelin density and cannot evaluate myelin relaxation times such as T_1 and T_2^* .¹²

Previous studies suggest that UTE type sequences with TEs of tens of microseconds can detect signal from myelin.^{8–10,13–16} Larson et al. proposed UTE imaging with long T_2 saturation for direct myelin imaging.¹³ The use of long- T_2 suppression pulses reveals a short T_2 component, which is believed to be associated with myelin in white matter that is obscured without suppression. Weiger et al. proposed a novel technique called *hybrid filling* for improved scan efficiency in zero TE (ZTE) imaging of myelin.¹⁴ Subtraction of two hybrid filling data with TEs of 15 μ s and 503 μ s provide high-contrast imaging of myelin. Boucneau et al. developed a UTE relaxometry acquisition strategy and fitting procedure for robust measurements in the presence of ultrashort T_2^* relaxation times and large frequency shifts.¹⁵ More recently, Shen et al. proposed 3D dual-echo UTE with a rosette k-space pattern for myelin imaging.¹⁶ The rosette k-space trajectory is based on rotations of a “petal-like” pattern in the k_x – k_y plane, with oscillated extensions in the k_z -direction for efficient 3D coverage. Multiple dual-echo 3D rosette UTE data were acquired for bicomponent analysis of short T_2^* (myelin) and long T_2^* (water) relaxation times and fractions.

The major challenge in direct myelin imaging is the concurrent detection of various water components in white matter of the brain, considering that myelin has a

much lower signal than water in white matter and especially gray matter of the brain.¹⁷ The long T_2 saturation, subtraction, and multicomponent fitting techniques are sensitive to B_1 and B_0 inhomogeneities, leading to potential water contamination in myelin mapping.¹⁸ Adiabatic inversion pulse provides uniform inversion of long T_2 water magnetizations; however, the longitudinal magnetizations for ultrashort T_2 components such as myelin remain largely positive.^{18–20} The nulling of the water signal can be achieved by using an optimal TI. Adiabatic inversion recovery-prepared UTE (IR-UTE) sequences have been proposed for high-contrast imaging of myelin. The dual-echo IR-UTE sequence can detect signal from myelin using the first echo acquisition, and signal from water using the second echo.¹⁹ At the water signal null point or optimal TI, the second echo detects near zero signal from water, whereas the first echo provides selective myelin imaging. The longitudinal magnetization of water is negative when TI is below the water signal null point or positive when TI is above the water signal null point. Therefore, a phase transition is expected for water when TI is increased from below to above the optimal TI in IR-UTE imaging. Furthermore, the optimal TI and phase transition also depend on TR. It is known that white matter T_1 varies across the whole brain, even in healthy brains.²¹ Greater T_1 variations are expected due to pathological changes. In this study, we examined the effect of TR and TI on water phase transition and signal nulling in 3D dual-echo IR-UTE imaging of myelin in the white matter of the brain using a whole-body clinical 3 T MR scanner. Five ex vivo and five in vivo human brains were investigated in this exploratory study.

2 | METHODS

2.1 | Pulse sequence

The 3D dual-echo IR-UTE Cones sequence was implemented on a 3 T scanner (MR750, GE Healthcare, Milwaukee, WI). Figure 1A shows the sequence that employs an adiabatic inversion pulse (Silver-Hoult, with a pulse duration of 6.048 ms, a bandwidth of 1.643 kHz, and a maximum B_1 amplitude of 17 μ T) for magnetization preparation, a short rectangular RF pulse (duration \sim 50 μ s) for nonselective excitation, and center-out 3D spiral trajectories for dual-echo k-space sampling.²² The first echo is sampled immediately after the RF excitation with a minimal nominal TE of 32 μ s, providing a FID sampling to detect signal from myelin and water components. The second gradient echo with a TE of \sim 2 ms detects signal from water components, with myelin signal decaying to the noise level.

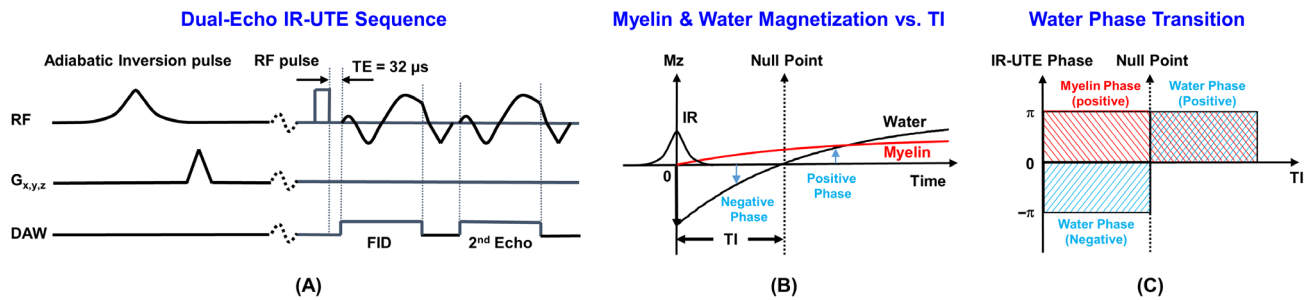


FIGURE 1 The 3D dual-echo IR-UTE sequence employs an adiabatic inversion pulse for water suppression, followed by a dual-echo Cones data acquisition with a minimal TE of $32\ \mu\text{s}$ for the FID sampling and a longer TE of $\sim 2\ \text{ms}$ for the second gradient echo sampling (A). The contrast mechanism in dual-echo IR-UTE imaging of myelin in white matter of the brain, where the adiabatic inversion pulse inverts the longitudinal magnetization of water and largely saturates the longitudinal magnetization of myelin (B). Selective myelin imaging can be achieved when UTE data acquisition starts at a TI when the inverted water magnetization approaches the null point. The water magnetization remains negative (negative phase) when TI is below the null point, and positive (positive phase) when TI is above the null point. Whereas the myelin phase remains positive, a water phase transition is expected for TI around the null point (C).

Figure 1B illustrates the contrast mechanism for direct myelin imaging using the 3D IR-UTE sequence. The relatively long adiabatic inversion pulse largely saturates the longitudinal magnetization of myelin because its duration is more than 10 times longer than the T_2 relaxation time of myelin.²⁰ Meanwhile, the water magnetization is uniformly inverted by the adiabatic inversion pulse as long as the adiabatic condition is met. Selective imaging of myelin can be achieved by UTE FID acquisition at the optimal TI when the inverted water magnetization approaches the null point.¹⁹ When TI is below the water signal null point, the longitudinal water magnetization is negative, producing a negative phase in the second echo of the dual-echo IR-UTE images. Positive longitudinal magnetization and phase are expected when TI is above the water signal null point. Myelin is expected to have a positive phase independent of TI. Therefore, a phase transition is expected for water signal in the second echo when TI is increased from below to above the optimal TI in dual-echo IR-UTE imaging. Figure 1C further illustrates this water phase transition, with myelin phase remaining positive for all TIs.

2.2 | Data acquisition

A 12-channel head coil was used for signal reception, and the body coil was used for signal excitation. The field map (B_0 map) and the B_1 phase map were derived from a three-echo Cones acquisition with TEs of 0.032, 2.2, and 4.4 ms (Figure 2).²³ The 3D dual-echo IR-UTE sequence was applied to five ex vivo human brain specimens and five healthy volunteers. The cadaveric human brain specimens were from the National Disease Research Interchange, which is the nation's leading source of human tissues, organs, and cells for research. The brain specimens were procured with a recovery to preservation interval

of less than 24 h. During MRI, each brain specimen was soaked in diluted formaldehyde (5% formalin to slow down tissue fixation or T_1 changes during scanning). After imaging, each specimen was soaked in 10% formalin for future histology studies. The sequence parameters for ex vivo 3D dual-echo IR-UTE imaging were: FOV = 22 cm, acquisition matrix size = 140×140 , sampling bandwidth = 166 kHz, number of slices = 48, slice thickness = 3 mm, TR = 500 ms, TE = 0.032 and 2.2 ms, flip angle = 28° , 6 to 8 TIs ranging from 160 to 200 ms, with a scan time of 5.5 min for each TI. Healthy volunteers were recruited following guidelines issued by our institutional review board. A total of five healthy volunteers (mean age: 28 ± 5 years, one female and four males) underwent the MRI scans. The inclusion criteria for the healthy controls were that participants were in good health and over 18 years old. Individuals with any contraindications to MRI were excluded from participation in the study. Written informed consent, which the institutional review board-approved, was obtained before each subject's participation. The sequence parameters for in vivo imaging were similar to the ex vivo study but with a thicker slice of 5 mm, a smaller number of slices of 32, and a shorter scan time of 2.5 min for each TI. A shorter TR of 106 ms was also tested, with five TIs of 44, 46, 48, 50, and 52 ms. Whiter matter T_1 was measured using a clinical 2D IR fast spin echo sequence with a TR of 5000 ms and six TIs of 50, 200, 400, 600, 1000, 1500, and 2000 ms.

2.3 | Data analysis

Both magnitude and phase images were generated for the dual-echo IR-UTE data. Phase unwrapping was applied to the UTE FID and the second gradient echo images. A region-growing-based algorithm was

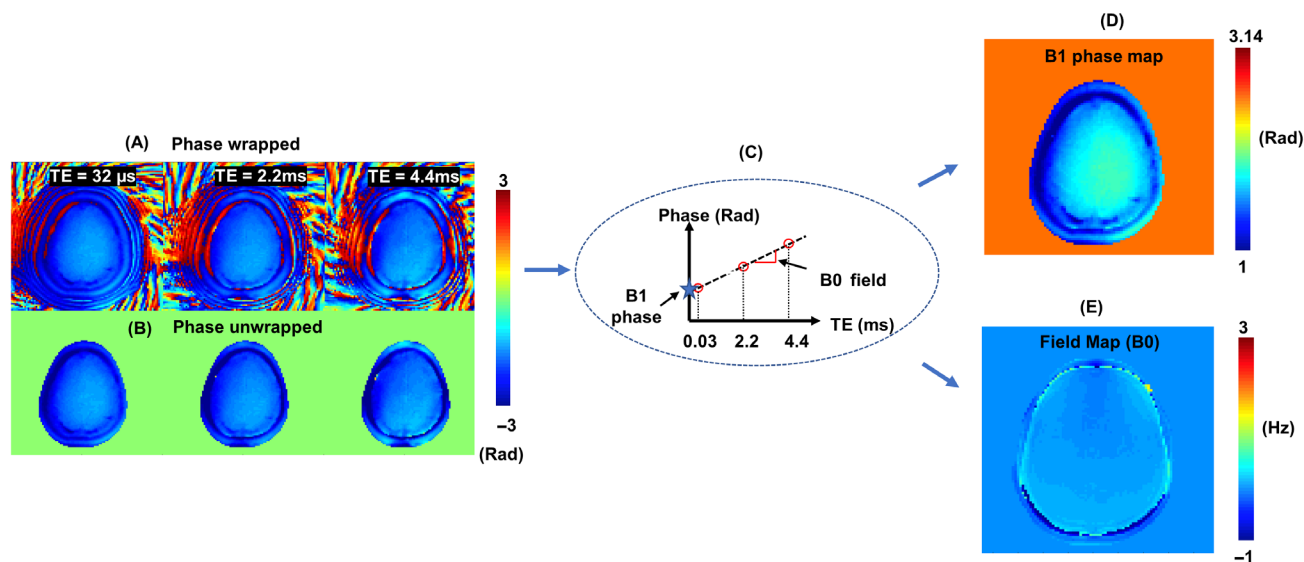


FIGURE 2 The B_0 and B_1 phase correction scheme is demonstrated on a normal brain (30-year-old female subject). Unwrapping of UTE phase map using field map (B_0) and phase map (B_1) estimated as slope and y-intercept after linear fitting of UTE phase maps acquired at three TEs of 0.032, 2.2, and 4.4 ms. Phase-wrapped images (A) at different echoes are unwrapped (B) using the algorithm illustrated in (C). The resultant phase maps for B_1 and B_0 are shown in (D) and (E), respectively.

implemented for phase unwrapping to obtain the global frequency shift (Figure 2).²³ A roll-off filter was designed to increase the contrast of phase images while suppressing high-frequency components prevalent in the outer k-space.²⁴ The Berkeley Advanced Reconstruction Toolbox was used to perform nonuniform fast Fourier transform–based reconstruction for the acquired UTE FID and gradient echo images.²⁵ The reconstructed images with data acquired by individual receive channels were combined to form a complex image. Data analysis was performed using MatLab 2021a (MathWorks, Natick, MA). Subtraction of the second echo from the UTE FID data was performed. The second echo phase and magnitude signal as a function of TI were plotted to investigate the water phase transition.

3 | RESULTS

Figure 2 shows the B_0 and B_1 correction after phase unwrapping. A linear fitting was used to identify the B_0 and B_1 phase maps derived from three TEs of 0.032, 2.2, and 4.4 ms (Figure 2C). The slope of fitting line was determined as the B_0 field map (Figure 2D), whereas the intercept was estimated as the B_1 map (Figure 2E). Figure 2B shows the phase images obtained from the reconstructed second echo of the 3D dual-echo IR-UTE data after B_0 and B_1 correction.

Magnitude and phase images of an ex vivo brain sample (female, 70-year-old donor) are shown in Figure 3.

Magnitude and phase images are displayed for both the first UTE FID and the second gradient echo with TIs ranging from 160 to 180 ms. A sharp phase transition was observed at a TI of ~ 178 ms, indicating the optimal nulling time for long- T_2 water components as shown in the Figure 3B. Phase change from the image at the shortest TI to the longest TI is presented in the Figure 3C, whereas the signal intensity is plotted in Figure 3D. Subtraction of the second echo from the UTE FID provides high-contrast imaging of myelin, as shown in the last row of Figure 3A.

Figure 4 shows the dual-echo magnitude images as well as B_0 - and B_1 -corrected phase maps of the brain of a 30-year-old healthy volunteer with a TR of 500 ms and six different TIs of 160, 170, 175, 180, 190, and 200 ms. All white matter regions show apparent water phase transition. However, water phase transition in the anterior region happened at a longer TI (190 ms vs. 180 ms) than in the posterior region. The second echo also shows the minimal signal intensity at a longer TI in the anterior region than in the posterior region of the brain (Figure 4C), which is consistent with the water phase transition shown in Figure 4B. This regional difference in water signal nulling is attributed to white matter T_1 variation across the whole brain (733 ± 26 ms for the anterior region vs. 700 ± 29 ms for the posterior region), which is a major challenge in selective myelin mapping. This T_1 variation is less problematic when a shorter TR is used, as shown in Figure 5. With a TR of 106 ms, the IR-UTE acquisition efficiently suppressed all water components, as demonstrated by the uniform phase transition for long- T_2 white matter seen

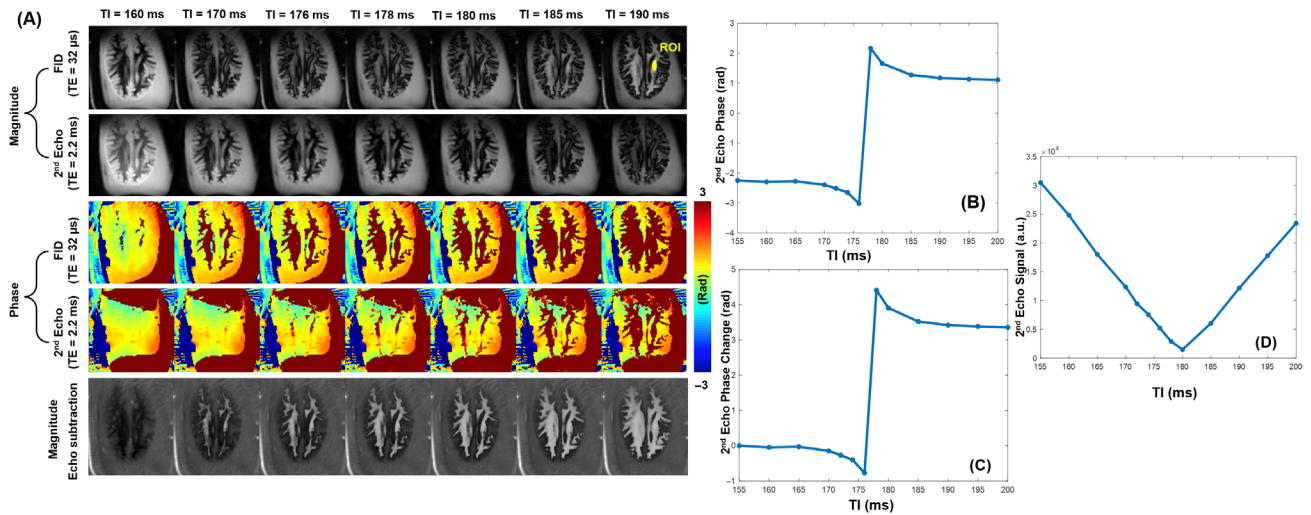


FIGURE 3 Representative magnitude and phase images for dual-echo IR-UTE imaging of an ex vivo human brain specimen with a TR of 500 ms and seven TIs of 160, 170, 176, 178, 180, 185, and 190 ms (A). A sharp water phase transition was observed at a TI of 180 ms for a ROI drawn in white matter of the brain (B). Phase change with respect to shortest TI (TI of 155 ms) is shown in (C). The second echo also reached the minimal signal intensity for the same ROI at the same TI of 180 ms, consistent with the water signal being nulled (D). Subtraction of the second echo from the first UTE FID produced high-contrast imaging of myelin (the last row in A).

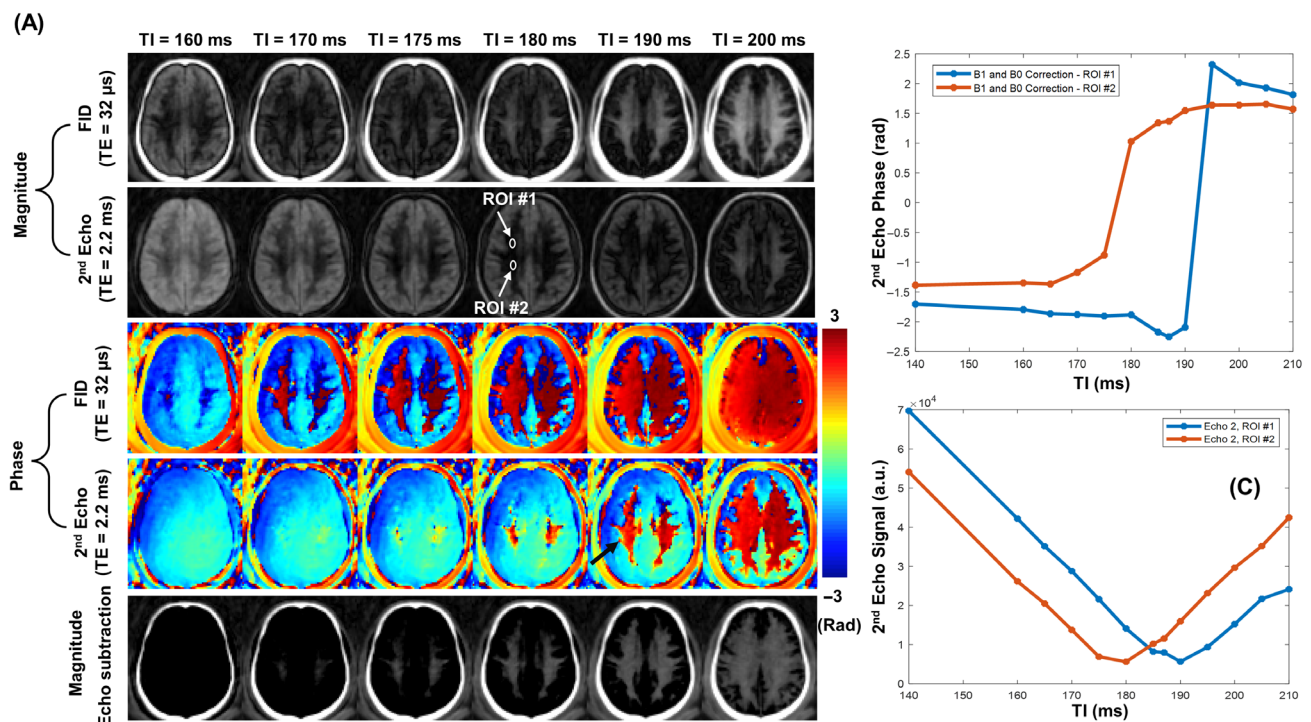


FIGURE 4 Representative magnitude and phase images for 3D dual-echo IR-UTE imaging of a 30-year-old healthy volunteer with a TR of 500 ms and six TIs of 160, 170, 175, 180, 190, and 200 ms (A). A sharp water phase transition was observed at a TI of 175 ms for ROI #1 and 190 ms for ROI #2 (B). The second echo showed a minimal signal intensity for ROI #1 at TIs of 175–180 ms, and for ROI #2 at a TI of 190 ms (C). The difference in water phase transition and signal null is due to T_1 variation with a longer T_1 of 733 ± 26 ms for ROI #1 and 700 ± 29 ms for ROI #2.

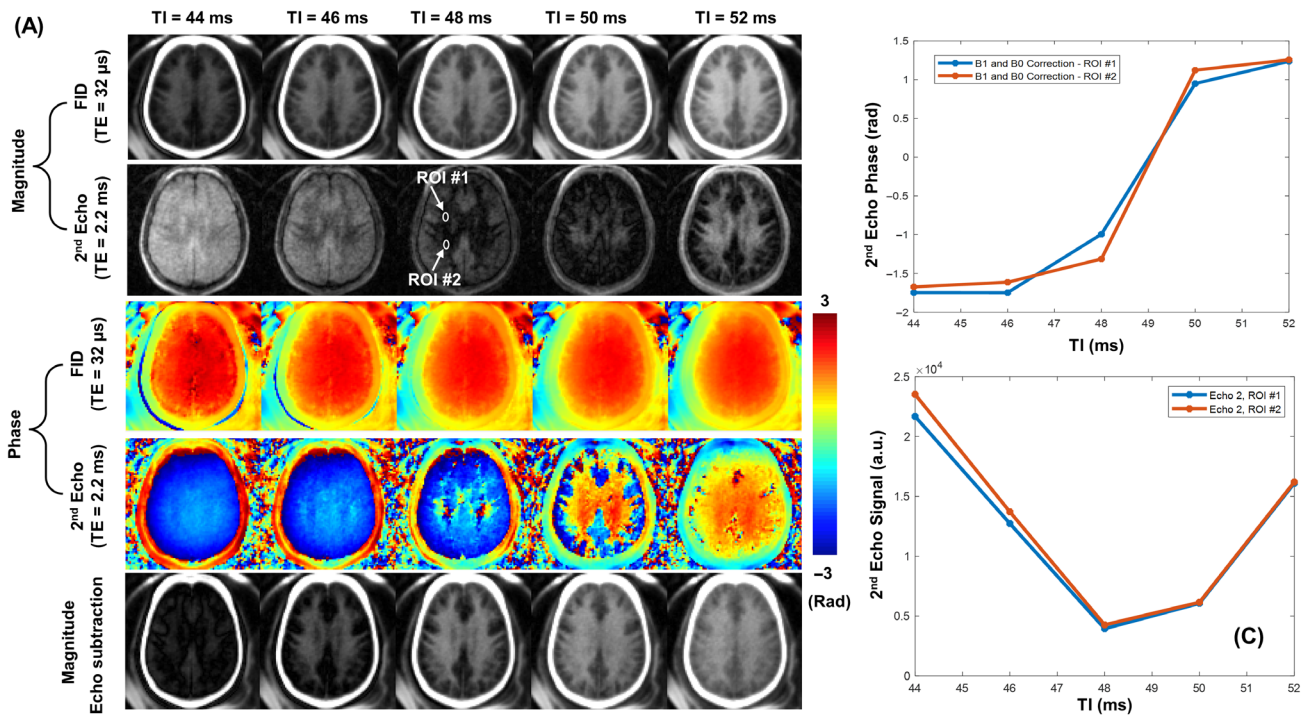


FIGURE 5 Representative magnitude and phase images for 3D dual-echo IR-UTE imaging of a 28-year-old healthy male volunteer with a TR of 106 ms and five TIs of 44, 46, 48, 50, and 52 ms (A). A sharp water phase transition was observed at a TI of 48 ms for both ROI #1 and ROI #2 (B). The second echo showed a minimal signal intensity for both ROI #1 and ROI #2 at the same TI of 48 ms (C). Whole brain myelin mapping is achieved by subtraction of the second echo from the UTE FID data collected at a TI of 48 ms (the last row in A).

from the corrected phase maps and magnitude images of a 28-year-old volunteer. Both water phase transition and long T_2 water signal nulling were observed at a TI of 48 ms (Figure 5B,C). Whole brain myelin mapping can be achieved regardless of T_1 variation.

Figure S1 provides the representative water phase transition plots for both TRs (500 ms and 106 ms) in 8 different white matter regions that include left and right subcortical white matter, centrum semiovale, periventricular regions, splenium and genu of the corpus callosum. It is observed that the shorter TR has a sharp transition for the phase signal compared to the long TR. Figure S2 demonstrates the water phase transition for the uncorrected images at the two different ROIs. Phase plots for both long TR and short TR are shown at different TIs. Figure S3 presents the quantification of T_1 measurements using the IR-FSE approach for various ROIs. Regional variations are observed from the different ROIs located in the white matter region.

4 | DISCUSSION

This study investigated the water phase transition and signal nulling in 3D dual-echo IR-UTE imaging of myelin in white matter of the brain *ex vivo* and *in vivo*. The effects of TI and TR were investigated by repeating dual-echo

IR-UTE data acquisition with a series of TIs and TRs. A sharp phase transition was demonstrated for long- T_2 white matter in dual-echo IR-UTE imaging of the brain when TI was increased from below to above the water signal null point. This water phase transition coincided with the second echo approaching the minimum signal intensity (i.e., the water signal null point). UTE FID data acquired at the corresponding TI is expected to provide selective imaging of myelin with water signal efficiently suppressed. Furthermore, the water phase transition point or optimal TI varied significantly across the brain when a relatively long TR (e.g., 500 ms) was used, precluding whole brain myelin mapping. A shorter TR (e.g., 106 ms) reduces the sensitivity to T_1 variation across the brain, allowing whole brain myelin mapping using a single TI (e.g., 48 ms).

Results from this study are also helpful for deeper understanding of the contrast mechanism in IR-UTE imaging of myelin. Waldman et al. reported 2D dual-echo IR-UTE imaging of myelin in white matter of the brain at 1.5 T using a very long TR of 2500 ms and a TI of ~ 360 ms for water suppression.¹⁹ Du et al. reported 2D dual-echo IR-UTE imaging of myelin at 3 T using a slightly reduced TR of 1000 ms and TI of ~ 330 ms for water suppression.²⁶ Wilhelm et al. reported 3D dual-echo IR-UTE imaging of myelin in rat thoracic spinal cord samples using a 9.4 T

vertical-bore spectrometer (Bruker DMX 400, Germany) with a TR of 1000 ms and TI of 500 ms, where the TI is suboptimal because the second echo ($TE = 1.2$ ms) showed strong residual signal from water components in white matter regions.⁹ Likely, all these sequences provide significant water contamination due to inaccurate TI and/or T_1 variation across the white matter regions.

Our results were consistent with the recent study by Ma et al., who reported a short repetition time adiabatic inversion recovery UTE (STAIR-UTE) sequence for whole brain myelin mapping.²⁷ Numerical simulation results suggest that a broad range of long T_2 signals with different T_1 s can be effectively suppressed when TR is less than 250 ms, with better long T_2 signal suppression for shorter TRs. The STAIR-UTE sequence can accurately quantify myelin concentration in myelin- D_2O phantoms ($T_2^* \sim 0.25 \pm 0.03$ ms), while efficiently suppressing signals from long T_2 agar phantoms (with different T_1 s) when TR is less than 250 ms. In contrast, signals in most phantoms and the agarose gel appeared bright on STAIR-UTE images when a long TR of 800 ms was used. A longer TR leads to higher sensitivity to T_1 variation in IR-UTE imaging. This T_1 sensitivity also explains the distinct water phase transition in the anterior region versus the posterior region of the brain as shown in Figure 4C, where a longer TI is required to null long T_2 water magnetization in the anterior region with longer T_1 than the posterior region. The STAIR-UTE sequence minimizes the effect of T_1 variation across the whole brain, providing robust whole brain myelin mapping. This is also confirmed by the uniform T_2^* values of whole brain white matter, ranging from 0.22 to 0.25 ms for eight white matter regions (left and right centrum semiovale, subcortical white matter, periventricular regions, as well as splenium and genu of corpus callosum).²⁷ When a TR of 106 ms was used, water phase transition and long T_2 signal nulling were observed at a TI of 48 ms for all white matter regions, suggesting that whole brain myelin mapping can be achieved with this short TR/TI combination. Theoretically, the shortest TR operated with specific absorption rate limits for clinical brain imaging would provide the most uniform water signal suppression.

Another approach for robust myelin mapping is the double-echo sliding IR-UTE technique,²⁸ which samples enough continuous image spokes to cover a wide range of TIs. A sliding window reconstruction is employed to generate one image per spoke, with up to 71 images, each of which has a different TI. The longitudinal magnetizations of long T_2 white matter can be nulled with an appropriate TI for each voxel, thereby providing robust selective imaging of myelin in white matter of the whole brain in different regions and different subjects despite variations in their T_1 s. The drawback of the double-echo sliding IR-UTE technique is that most of the spokes are sampled

at nonoptimal TIs, leading to a low acquisition efficiency for myelin mapping. In contrast, all spokes in STAIR-UTE imaging are sampled at the optimal TI and can be used to generate myelin maps.

The IR-based UTE techniques are expected to be more robust for myelin mapping than long T_2 saturation, echo subtraction, and bicomponent or multicomponent fitting techniques.¹⁸ Adiabatic inversion pulse provides uniform inversion of long T_2 water magnetizations, allowing perfect nulling of water signal if an optimal TI is used. The long T_2 saturation technique is sensitive to B_1 field inhomogeneity, which leads to varied saturation flip angles and, thus, residual long T_2 water signal contamination. The B_0 field inhomogeneity is another major confounding factor, affecting not only the long T_2 saturation technique but also the echo subtraction, bicomponent, and multicomponent fitting techniques.²⁹ The adiabatic inversion pulse with a relatively broad spectral bandwidth is insensitive to B_1 and B_0 inhomogeneities,²⁰ providing uniform inversion of long T_2 water components in the whole brain. T_1 variation is the only confounding factor, which can be resolved by using a short TR. As a result, IR-UTE imaging with a short TR, or STAIR-UTE, allows robust long T_2 suppression, providing selective whole brain myelin mapping. Water contamination due to regional- or pathological-related T_1 variations can be minimized.

There are several limitations to this study: First, only a small number of TIs and a relatively low number of TRs were investigated on the effect of water phase transition and signal suppression in IR-UTE imaging of myelin due to scan time limitation. However, the general trend holds that water phase transition and signal nulling coincide with the optimal TI. Second, no absolute evidence is provided to demonstrate that the IR-UTE signal at the optimal TI is solely from myelin in the ex vivo and in vivo brain studies. Our prior studies on STAIR-UTE imaging of the brain in vivo showed an ultrashort T_2^* of ~ 0.22 ms,²⁷ which is very close to the T_2^* of ~ 0.16 ms for lyophilized myelin powder.¹⁰ This result indirectly confirms that myelin is a major signal source in IR-UTE imaging, especially when a short TR is used. Third, in order to compensate for the B_0 and B_1 field inhomogeneities, additional sequences were acquired for B_0 and B_1 phase maps that increased the total scan time. Fourth, myelin in gray matter was not investigated in this work. It is already challenging to acquire myelin signal in white matter of the brain due to the low proton density and ultrashort short T_2 of myelin protons. Gray matter has significantly lower myelin content, which makes it even more challenging for direct imaging using the dual-echo IR-UTE sequence on a clinical whole-body scanner. IR-UTE imaging of myelin at higher field strength, such as 7 T,^{15,30} can potentially be used for more robust mapping of myelin in white matter and potentially gray matter. Fifth, the

number of ex vivo specimens and in vivo subjects is relatively small, demonstrating feasibility but derailing the statistical significance.

5 | CONCLUSION

Our results suggest a sharp water phase transition and signal null near the optimal TI in dual-echo IR-UTE imaging of myelin in white matter of the brain. The water phase transition point or optimal TI varied significantly across the brain when a relatively long TR. IR-UTE imaging with a shorter TR provides uniform water phase transition at the optimal TI, allowing robust whole brain myelin mapping.

ACKNOWLEDGMENTS

The authors acknowledge grant support from the National Institutes of Health (RF1 AG075717, F32AG082458) and the Clinical Science Research & Development (I01CX002211).

ORCID

Jiyo S. Athertya  <https://orcid.org/0000-0002-0866-1052>

Soo Hyun Shin  <https://orcid.org/0000-0003-1875-2908>

Hyungseok Jang  <https://orcid.org/0000-0002-3597-9525>

Yajun Ma  <https://orcid.org/0000-0003-0830-9232>

REFERENCES

- Felts PA, Baker TA, Smith KJ. Conduction in segmentally demyelinated mammalian central axons. *J Neurosci*. 1997;17:7267-7277.
- Chabas D, Baranzini SE, Mitchell D, et al. The influence of the proinflammatory cytokine, osteopontin, on autoimmune demyelinating disease. *Science*. 2001;294:1731-1735.
- Fünfschilling U, Supplie LM, Mahad D, et al. Glycolytic oligodendrocytes maintain myelin and long-term axonal integrity. *Nature*. 2012;485:517-521.
- Lee Y, Morrison BM, Li Y, et al. Oligodendroglia metabolically support axons and contribute to neurodegeneration. *Nature*. 2012;487:443-448.
- van der Knaap MS, Valk J. Magnetic resonance of myelination and myelin disorders. *J Neuroradiol*. 2006;33:132.
- Lee J, Hyun JW, Lee J, et al. So you want to image myelin using MRI: an overview and practical guide for myelin water imaging. *J Magn Reson Imaging*. 2021;53:360-373.
- Laule C, Vavasour IM, Kolind SH, et al. Magnetic resonance imaging of myelin. *Neurotherapeutics*. 2007;4:460-484.
- Horch RA, Gore JCDM. Origins of the ultrashort-T2 1H NMR signals in myelinated nerve: a direct measure of myelin content? *Magn Reson Med*. 2011;66:24-31.
- Wilhelm MJ, Ong HH, Wehrli SL, et al. Direct magnetic resonance detection of myelin and prospects for quantitative imaging of myelin density. *Proc Natl Acad Sci U S A*. 2012;109:9605-9610.
- Sheth V, Shao H, Chen J, et al. Magnetic resonance imaging of myelin using ultrashort echo time (UTE) pulse sequences: phantom, specimen, volunteer and multiple sclerosis patient studies. *Neuroimage*. 2016;136:37-44.
- Barkhof F. The clinico-radiological paradox in multiple sclerosis revisited. *Curr Opin Neurol*. 2002;15:239-245.
- Ma YJ, Jang H, Chang EY, et al. Ultrashort echo time (UTE) magnetic resonance imaging of myelin: technical developments and challenges. *Quant Imaging Med Surg*. 2020;10:1186-1203.
- Larson PEZ, Gurney PT, Nayak K, Gold GE, Pauly JM, Nishimura DG. Designing long-T2 suppression pulses for ultrashort echo time imaging. *Magn Reson Med*. 2006;56:94-103.
- Weiger M, Froidevaux R, Baadsvik EL, Brunner DO, Rösler MB, Pruessmann KP. Advances in MRI of the myelin bilayer. *Neuroimage*. 2020;217:116888.
- Boucneau T, Cao P, Tang S, et al. In vivo characterization of brain ultrashort-T2 components. *Magn Reson Med*. 2018;80:726-735.
- Shen X, Özen AC, Sunjar A, et al. Ultra-short T2 components imaging of the whole brain using 3D dual-echo UTE MRI with rosette k-space pattern. *Magn Reson Med*. 2023;89:508-521.
- Fan SJ, Ma Y, Zhu Y, et al. Yet more evidence that myelin protons can be directly imaged with UTE sequences on a clinical 3T scanner: Bicomponent T2* analysis of native and deuterated ovine brain specimens. *Magn Reson Med*. 2018;80:538-547.
- Ma Y, Jang H, Jerban S, et al. Making the invisible visible—ultrashort echo time magnetic resonance imaging: technical developments and applications. *Appl Phys Rev*. 2022;9:041303.
- Waldman A, Rees JH, Brock CS, Robson MD, Gatehouse PD, Bydder GM. MRI of the brain with ultra-short echo-time pulse sequences. *Neuroradiology*. 2003;45:887-892.
- Larson PEZ, Conolly SM, Pauly JM, Nishimura DG. Using adiabatic inversion pulses for long-T2 suppression in ultrashort echo time (UTE) imaging. *Magn Reson Med*. 2007;58:952-961.
- Ethofer T, Mader I, Seeger U, et al. Comparison of longitudinal metabolite relaxation times in different regions of the human brain at 1.5 and 3 Tesla. *Magn Reson Med*. 2003;50:1296-1301.
- Carl M, Bydder GM, Du J. UTE imaging with simultaneous water and fat signal suppression using a time-efficient multipole inversion recovery pulse sequence. *Magn Reson Med*. 2016;76:577-582.
- Cusack R, Papadakis N. New robust 3-D phase unwrapping algorithms: application to magnetic field mapping and undistorting echoplanar images. *Neuroimage*. 2002;16:754-764.
- Pipe JG. Reconstructing MR images from undersampled data: data-weighting considerations. *Magn Reson Med*. 2000;43:867-875.
- Martin U, Frank O, Jonathan T, et al. Berkeley advanced reconstruction toolbox. In Proceedings of the 23rd Annual Meeting of ISMRM, Toronto, Ontario, Canada, 2015. p. 2486.
- Du J, Ma G, Li S, et al. Ultrashort echo time (UTE) magnetic resonance imaging of the short T2 components in white matter of the brain using a clinical 3T scanner. *Neuroimage*. 2014;87:32-41.
- Ma YJ, Jang H, Wei Z, et al. Myelin imaging in human brain using a short repetition time adiabatic inversion recovery prepared ultrashort echo time (STAIR-UTE) MRI sequence in multiple sclerosis. *Radiology*. 2020;297:392-404.

28. Ma YJ, Searleman AC, Jang H, et al. Whole-brain myelin imaging using 3D double-echo sliding inversion recovery ultrashort echo time (DESIRE UTE) MRI. *Radiology*. 2020;294:362-374.
29. Du J, Bydder M, Takahashi AM, Carl M, Chung CB, Bydder GM. Short T2 contrast with three-dimensional ultrashort echo time imaging. *Magn Reson Imaging*. 2011;29:470-482.
30. Müller M, Egger N, Sommer S, et al. Direct imaging of white matter ultrashort T2* components at 7 Tesla. *Magn Reson Imaging*. 2022;86:107-117.

SUPPORTING INFORMATION

Additional supporting information may be found in the online version of the article at the publisher's website.

FIGURE S1. Representative water phase transition plots for different ROIs including the left and right subcortical white matter, centrum semiovale, periventricular regions, splenium and genu of the corpus calosum, placed in the white matter region of two healthy controls. (A) 30 year old healthy volunteer with a TR of 500 ms shows abrupt phase transitions owing to regional T1 variation while (B)

shows phase plots from a 28 year old healthy control at TR = 106 ms. It is noted that shorter TR has a sharp phase transition compared to longer TR.

FIGURE S2. Water phase transition using the uncorrected images (without B0/B1 correction) at two different ROIs. (A) presents the phase plot at longer TR while (B) shows the shorter TR phase transitions obtained at different TIs.

FIGURE S3. Quantification of T1 measurements at different ROIs using the IR-FSE approach. Regional variation in the T1 values is observed from the different ROIs placed in the white matter region.

How to cite this article: Athertya JS, Shin SH, Malhi BS, et al. Water phase transition and signal nulling in 3D dual-echo adiabatic inversion-recovery UTE (IR-UTE) imaging of myelin. *Magn Reson Med*. 2024;92:2464-2472. doi: 10.1002/mrm.30243